

# **Experimental study of historical processing of cobalt arsenide ore for colouring glazes (15-16th century Europe)**

Judit Molera<sup>(1)\*</sup>, Aurelio Climent-Font<sup>(2)</sup>, Gaston Garcia<sup>(2,3)</sup>, Trinitat Pradell<sup>(4)</sup>, Oriol Vallcorba<sup>(3)</sup>, Alessandro Zucchiatti<sup>(5)</sup>

<sup>1)</sup> MECAMAT. Faculty of Sciences and Technology. University of Vic – Central University of Catalonia. C. de la Laura, 13, 08500 Vic, Catalonia

<sup>2)</sup> Universidad Autónoma de Madrid, Centro de Microanálisis de Materiales, calle de Faraday 3, 28049, Madrid, Spain

<sup>3)</sup> ALBA Synchrotron Light Source, Carrer de la Llum 2-26, 08290 Cerdanyola del Vallès, Barcelona, Spain

<sup>4)</sup> Universitat Politècnica de Catalunya, Departament de Física, BRCMSE, campus Diagonal-Besòs, Av. Eduard Maristany 17, 08019, Barcelona, Spain

<sup>5)</sup> University of the Witwatersrand, School of Physics, Private bag 3, WITS 2080, Johannesburg, South Africa

## **Abstract**

Cobalt was used since the early antiquity to tint glass and glazes in blue. The presence of arsenic in blue decorated glazes since ~1500 onwards and absence beforehand, observed in Europe, might be related to the processing of the ore: roasting of the cobalt mineral (*saffre*) and obtaining a glass adding sand and potash (*smalt*) or as by-product of other metallurgical processes, e.g. silver smelting slag. We have replicated the roasting of cobalt arsenide ore ( $\text{CoAs}_3$ ) and the processing of silver smelting as described in historical treatises following the transformations by *in situ* variable temperature SR-XRD, PIXE and SEM. Our laboratory tests have proved that roasting cobalt arsenide ore either alone or mixed with fluxes ( $\text{PbO}$ ,  $\text{CaF}_2$ ),  $\text{CaCO}_3$ ,  $\text{SiO}_2$  and kaolinite was unable to remove the arsenic completely. Roasting cobalt arsenide ore (*saffre*) alone explains the presence of arsenic in the cobalt blue glasses and glazes after 1520. The product obtained as described by Agricola contains less arsenic forming calcium arsenates, lead arsenates ( $\text{Pb}_5(\text{AsO}_4)_3\text{F}$ ,  $\text{Pb}_8\text{As}_2\text{O}_{13}$ ) and calcium lead arsenates  $(\text{Ca,Pb})_5(\text{AsO}_4)_3(\text{F,Cl,OH})$  with an hedyphane structure, while cobalt is incorporated into a glassy matrix. As the physical separation of the arsenic free cobalt vitreous phase does not seem possible, these processes can explain the variable content of arsenic shown by the historical blue glazes but not the arsenic free glazes. In this case, the use of an arsenic free cobalt ore such as linnaeite is the most likely source.

**Keywords:** skutterudite, cobalt pigments, blue glazes, calcium lead arsenate, roasting  $\text{CoAs}_3$ , *saffre*

\* Corresponding author  
Judit Molera

## 1-INTRODUCTION

Cobalt was used since the early antiquity to tinge glass and glazes in blue. The chemical composition of blue glasses and glazes from various regions and different epochs has been extensively studied. An instrumental study of glass from French archaeological sites (Gratuze et al., 1992; Soulier et al., 1996) and of ceramics from France, Italy, Spain, Maghreb, Uzbekistan, Syria and Egypt (Gratuze et al., 1996) has identified three major groups of cobalt pigments and gave hints on the origin and processing of cobalt ore:

- The first group is characterized by the presence of Co, Zn, Pb and In (min 19 - max 587 ppm), with high concentration of zinc and lead. It includes objects dated from the beginning of 13<sup>th</sup> to the end of the 15<sup>th</sup> century. The village of Freiberg in the Erzgebirge, where cobalt minerals are associated with zinc blend and galena, has been suggested by the authors (Gratuze et al., 1992) as the possible source.
- The second group shows only the association of Co and Ni (Co/Ni ~ 4) with very low As content (min 58 - max 687 ppm) and includes objects dated from around the end of the 15<sup>th</sup> and the beginning of 16<sup>th</sup> century. The authors suggest that it might be the result of a higher temperature roasting of cobalt arsenates or sulpho-arsenates.
- The third group is characterized by the presence of Co and Ni (Co/Ni ~ 4), a high concentration of As (~20 times those of group 2) and Bi, and includes objects dated from the beginning of 16<sup>th</sup> century onward. This kind of pigment is associated with the *saffre* discussed below, probably from Schneeberg.

The analysis of ceramics (Gratuze et al., 1996, 2018; Pérez-Arantegui et al., 2008; Porter, 1997; Roldán et al., 2006) confirms so far these three groups. The analysis, by Particle Induced X-ray Emission (PIXE), of the blue glazes in objects of the della Robbia production, accurately dated from 1445 to 1550 (Zucchiatti et al., 2006a), allowed to add precision to the time scale. In the Della Robbia production the compositional change between the second and the third group takes place, sharply, between the years 1515 and 1521 (Pappalardo et al., 2004).

The differences in composition have given rise to several hypotheses about the origin of the cobalt ores and their processing, not all of which could be firmly confirmed. The presence of

70 arsenic from 1520 until the end of the 17<sup>th</sup> century suggests the use of the *saffre* produced as  
71 described by Kunckel in his “*Ars vitraria experimentalis*” published in 1679 (Kunckel, 1679).  
72 Kunckel details the *saffre* fabrication process with “*a metallic stone called cobalt*” which is very  
73 poisonous. It has to be roasted in a reverberatory oven, procuring that it emits light and a white  
74 smoke (arsenic), collected along a wooden horizontal chimney. The calcined material is milled into  
75 a fine powder. Part of the powder is mixed with quartz, moist and pressed inside a barrel to form  
76 a compound as hard as a stone. This material, that the miners and other authors call *Zaffera* (the  
77 *saffre*), is sent to Holland for the production of plates. Melzer (Melzer, 1684) refers to a specific  
78 person, *Peter Weidenhammer* from Schneeberg, as a producer of *Zaffera* and to a year, 1520, in  
79 which he had donated a window to the village great church. *Smalt*, invented around 1540–60, is a  
80 potassium glass obtained by melting the roasted cobalt ore together with quartz (sand) and potash  
81 or added to molten glass (Mühlethaler and Thissen, 1969, Bajnóczi, et al 2014).

82  
83 The peculiar Co-Ni group, identified by Soulier and coworkers (Soulier et al., 1996), that  
84 included objects dated before 1520, i.e. before the *saffre* was introduced, was attributed to  
85 roasting of a cobalt ore (like erythrite) at a higher temperature than those obtained in a  
86 reverberatory kiln. However, it is not clear if this could explain the drop in arsenic below PIXE  
87 detection limits and to the average 93 ppm given by ICP-MS. Looking at an arsenic free cobalt  
88 pigment, we cannot exclude, a priori, the possibility that such a material was obtained as a by-  
89 product of the silver smelting. In his treatise “*De re Metallica*” (Agricola, Hoover & Hoover, 2011),  
90 Georgius Agricola describes meticulously the silver production, from mining to purification of the  
91 metal but never mentions explicitly cobalt as a by-product. However, we know that the Erzgebirge  
92 silver comes in association with Co, Ni, Fe, As, Bi (Andrews, 1962, Kissin 1992). The exploitation of  
93 the Erzgebirge silver mines is documented since 1168 (Freiberg) and has been the major economic  
94 activity of the area until the 16<sup>th</sup> century. Cobalt ores may therefore be present in the smelting.  
95 We also know that cobalt has the tendency “...*to remain in the silicate melt until the closing stages*  
96 *of the magmatic differentiation... and this same tendency is manifest in the metallurgical*  
97 *operations when the cobalt is more likely to go into the slag*” (Andrews, 1962). The question is  
98 whether the metallurgic operations described by Agricola, would produce a separation of Co and  
99 As. For the sake of reproducing in laboratory tests the process he describes, it is worth considering  
100 some key sentences of Agricola’s text translation (Agricola, Hoover & Hoover, 2011).

101           “... he [the master smelter] first throws into the furnace as many cakes melted from pyrites [the  
102 metallurgical matte] as he requires to smelt the ore; then he puts in two wicker baskets full of ore  
103 with litharge and hearth-lead, and stones which fuse easily by fire of the second order, all mixed  
104 together; then one wicker basket full of charcoal, and lastly the slags. The furnace now being filled  
105 with all the things I have mentioned, the ore is slowly smelted”. “... when the lead which the  
106 assistant has placed in the forehearth is melted, the master opens the tap-hole of the furnace with  
107 a tapping-bar...The slag first flows from the furnace into the forehearth, and in it are stones mixed  
108 with metal or with the metal adhering to them partly altered, the slag also containing earth and  
109 solidified juices. After this, the material from the melted pyrites flows out, and then the molten  
110 lead contained in the forehearth absorbs the gold and silver. When that which has run out has  
111 stood for some time in the forehearth, in order to be able to separate one from the other, the  
112 master first either skims off the slags with the hooked bar or else lifts them off with an iron fork;  
113 the slags, as they are very light, float on the top. He next draws off the cakes of melted pyrites,  
114 which as they are of medium weight hold the middle place; he leaves in the forehearth the alloy of  
115 gold or silver with the lead, for these being the heaviest, sink to the bottom. As, however, there is  
116 a difference in slags, the uppermost containing little metal, the middle more, and the lowest much,  
117 he puts these away separately, ...”.

118

119           Being the cooling of the melt relatively fast in air and driven by sedimentation, we expect the  
120 heavy elements, like Bi, to go into the ingot with lead and silver, which would justify the  
121 appearance of Bi in the della Robbia glazes only in coincidence with the appearance of As, i.e.  
122 when the cobalt mineral is roasted as a whole and not melted and sedimented.

123

124           In this study we have thermally processed a cobalt arsenide ore, in order to replicate as close  
125 as possible the historical account of roasting (Kunckel, 1679) and we have as well thermally  
126 processed mixtures of cobalt arsenide ore and other compounds to reproduce the smelting  
127 process described by Agricola (Agricola, 1530). The purpose is to determine the nature of the  
128 products obtained from these processing and use the results to assess or deny the various  
129 hypotheses found in the literature about the effect that those processes had in the composition  
130 of the cobalt pigment, in particular those regarding the partial or complete loss of arsenic.

131

132

## 2- EXPERIMENTAL METHODOLOGY

A cobalt arsenide ore, originating from Ouarzazate mines (Ahmed 2009a) in Morocco (courtesy of the University Moulay Ismail of Meknes), was ground in agate mortar with granulometry below 80 microns: the biggest quartz and calcite grains were removed at an intermediate grinding stage. The mineral composition of the cobalt arsenide ore was determined by X-Ray Diffraction (XRD). The ore is an inhomogeneous aggregate of skutterudite ( $\text{CoAs}_3$ ) and a little clinosafflorite ( $\text{CoAs}_2$ ) with calcite ( $\text{CaCO}_3$ ), quartz ( $\text{SiO}_2$ ) and clinochlore ( $(\text{Mg}_5\text{Al})(\text{Si},\text{Al})_4\text{O}_{10}(\text{OH})_8$ ) as gangue minerals. Neither erythrite ( $\text{Co}_3(\text{AsO}_4)_2 \cdot 8\text{H}_2\text{O}$ ) nor cobaltite ( $\text{CoAsS}$ ) were detected (Table I). The average chemical composition of the cobalt ore was determined by PIXE (Particle Induced X-ray Emission) (Johansson et al., 1995), scanning a few millimetric portions of the grey and visually homogeneous ore areas and averaging the results. The PIXE analysis was performed with a 3 MeV, 30  $\mu\text{m}$  diameter, scanning external proton micro-beam at the AGLAE accelerator of the C2RMF (Calligaro et al., 2000). We collected X-rays with a two detector apparatus described in detail elsewhere (Zucchiatti et al., 2000). The average composition obtained for the mineral is: 63.4 wt% As, 14.3 wt% Co, 3 wt% Ni, 1.6 wt% Fe, 2.4 wt% S, 7.3 wt% Si, 5.3 wt% Ca, 1 wt % Na and 0.5 wt% Al. Magnesium could not be detected since its K line at 1.254 keV cannot be separated by the dominant L line of arsenic at 1.282 keV but SEM-EDS confirmed its presence in the clinochlore particles (Figure S1). Based on the elemental composition obtained by PIXE and assuming that all the Co, Ni, As and S and part of the Fe belong to the cobalt arsenide, all the Ca to calcite ( $\text{CaCO}_3$ ), all the Al and part of the Fe and Si to clinochlore, taking the composition measured by SEM-EDS (Scanning Electron Microscope-Energy Dispersive Spectroscopy) for the clinochlore,  $\text{Mg}_3\text{Fe}_2\text{Al}(\text{Si}_3\text{Al})\text{O}_{10}(\text{OH})_8$ , and the remaining Si to quartz, the mineral composition has been calculated to be about 71% cobalt arsenide, 12% calcite and 12%  $\text{SiO}_2$  and 5% clinochlore.

The cobalt ore was roasted alone to replicate the *saffre* production and mixed with other minerals (Table I) to mimic the mixtures that were introduced in the kiln during the silver smelting process as described by Agricola. The materials added were lead oxide ( $\text{PbO}$ ) and minium ( $\text{Pb}_3\text{O}_4$ ) (Sigma Aldrich ref. 203610 and ref. 241547, respectively) used as a flux, quartz ( $\text{SiO}_2$ ) (Sigma Aldrich ref. 204358), calcite ( $\text{CaCO}_3$ , Sigma Aldrich ref. 239216), kaolinite ( $\text{Al}_2\text{Si}_2\text{O}_5(\text{OH})_4$ ) (Supelco ref. 1044402500), possibly present in the kiln walls for the silver smelting process. Furthermore,

164 fluorite (CaF<sub>2</sub>) (Sigma-Aldrich ref. 449717) was added since Hoover (Agricola, Hoover & Hoover,  
165 2011) proposed it – with admitted difficulty and uncertainty – as the *stones which fuse easily by*  
166 *fire of the second order*. The mineral content of each mixture is given in Table S1 and the As, Co,  
167 Ni, Fe and S composition of each mixture is given in Table S2.

168  
169 To mimik the roasting and smelting two different procedures have been followed. In a first  
170 step a *static process* (SP) was adopted. We roasted/melted about 200 mg of cobalt ore or 1-2 g of  
171 the mixtures of Table I, inside alumina vessels, placed into a quartz tube, by means of an  
172 electronically controlled oven in a forced air flux. The temperature raised at a rate of 5°C/minute  
173 and was maintained at the set maximum value for a period of not less than 8 hours. The maximum  
174 temperatures were 460, 650, 850 and 1000 °C. Then the oven cooled down for 10 to 12 hours  
175 before the samples were extracted and analyzed by PIXE and SEM-EDS at the Centre de Recherche  
176 et Restauration des Musées de France (C2RMF).

177  
178 Given the results of the SP investigation, we planned a *dynamic process* (DP) for further study  
179 by SR-XRD (Synchrotron Radiation powder X-Ray Diffraction). The SR-XRD, time/temperature  
180 resolved, was performed at the ALBA synchrotron, in Cerdanyola del Vallès (Barcelona). Mixtures  
181 were ground in agate mortar with granulometry below 80 microns and 50 mg were inserted into  
182 500 µm diameter quartz capillaries and heated with an air blower, while performing powder X-ray  
183 diffraction. The experiment was carried on at the high-resolution station of the BL04-MSPD  
184 (Materials Science and Powder Diffraction) Beamline (Fauth et al., 2013). The diffracted X-rays  
185 were collected by the Mythen detector, composed of 6 modules (Dectris/PSI Detectors group)  
186 with a strip-pitch of 50 µm and placed at 550 mm of the sample, covering an angular range of 40°  
187 (2θ) with 2θ step of 0.6·10<sup>-2</sup>°. Sequential data collection was performed during the heating stage.  
188 During the cooling down of the samples, datasets were acquired as fast as compatible with a  
189 reasonable level of statistics, in such a way that structural changes during the cooling down could  
190 also be explored. In this case, the temperature intervals corresponding to each dataset are very  
191 large initially and become progressively smaller as the cooling rate moderates. The energy used  
192 for the measurements was 30 keV (wavelength λ=0.4129 Å, determined from a NIST640d silicon  
193 standard) which is convenient for the absorption of the samples, including those containing a high  
194 percentage of strong absorbing elements such as Pb. The flux on sample was  
195 about 4·10<sup>12</sup> photons/s and the beam size 2 x 0.8 mm<sup>2</sup> (WxH). The end station is equipped with a

196 holder that spins the capillary slightly tilted (5 degrees in our case) with respect to the horizontal  
197 plane to avoid powder loss while allowing gas escape from the open end. A FMB Oxford hot air  
198 blower controls the temperature growth rate from room temperature (RT) to 90°C at 20°C/min,  
199 90°C to 110°C at 5°C/min, 110°C to 400°C at 20°C/min and 400°C to 900°C at 10°C/min) and data  
200 collection time is kept constant (40 seconds/pattern). After reaching a top of 900 °C, the blower  
201 returns directly at RT, which is enough to produce a relatively fast cooling of the sample, mimicking  
202 the cooling down of the melt once the kiln tap-hole was open and the melt flowed in the fore-  
203 heart (Agricola, 1556).

204

205 Additional SR- $\mu$ XRD measurements have been performed after heating at RT along the  
206 capillaries, from the area heated by the blower to the edge and which correspond to progressively  
207 lower temperatures. The aim of these measurements was to help with the identification of the  
208 phases. These measurements were performed at the microdiffraction endstation of the same  
209 beamline using a 15x15 $\mu$ m<sup>2</sup> beam (FWHM) at 29.2keV (0.4246 Å wavelength) and a 2D CCD  
210 Rayonix SX165 detector. Moreover, a 17th century Catalan blue decorated glaze which contains  
211 calcium lead arsenate crystals, similar to those found in the roasted mixtures, were also analysed  
212 by SR- $\mu$ XRD (for more detail on sample preparation see Pradell et al. 2013). Crystals of this sample  
213 were also analysed by microprobe (WDS) at Universitat de Barcelona. The experimental conditions  
214 for WDS analysis were 15 kV and 15 nA and an electron beam size of 2 mm.

215

### 216 3. THE SAFFRE PRODUCTION PROCESS: LABORATORY TESTS

217

218 After roasting the cobalt arsenide ore alone, in the SP process, a white uniform surface layer  
219 covered the ore and the quartz tube into which the alumina vessel was placed. The grey ore was  
220 transformed into a black compound that was easily broken and showed a complex granular  
221 structure (**Figure S2**). The ore in its natural state, the calcined samples and the white patina were  
222 analysed by PIXE. The white patina was almost pure arsenic. Despite the As loss, the weight ratio  
223 As/Co of the roasted compounds dropped above 460 °C, but it never went below 1, not even at  
224 the highest roasting temperature of 1000 °C, as shown in **Figure 1**.

225

226 The *DP* of the cobalt ore alone (sample m1 of Table I) was run up to 900 °C. The diffractograms  
227 taken during the experiment are shown in **Figure 2**. The diffractogram at the top corresponds to

228 the raw cobalt ore, the green diffractogram is the one taken at 573 °C (quartz alpha to quartz beta  
229 transition) during heating, the red diffractogram is the one taken at the maximum temperature  
230 (900 °C) and the diffractogram at the bottom corresponds to the material obtained after firing  
231 measured at RT. Following the roasting we could state that skutterudite began to decompose in  
232 *DP* at 550°C, completely disappearing at 851°C (we should notice that the temperatures indicated  
233 are those at which the diffractogram patterns were taken). The presence of clinosafflorite, residual  
234 before firing, increases between 717oC and 900oC following the decomposition of skutterudite.  
235 Langisite, (Co,Ni)As, is also formed between 809°C and 900°C. Cobalt arsenate  $\text{Co}_3(\text{AsO}_4)_2$  is  
236 formed during heating at about 575°C and disappears at 790°C. The arsenic volatilised diffuses  
237 along the capillary and precipitates in the cooler regions as  $\text{As}_2\text{O}_3$  and also as metallic As (**Figure**  
238 **3**).

239  
240 With regard to the other minerals present in the ore, clinochlore decomposes at 650°C and  
241 calcite decomposes quickly between 850°C and 900°C and quartz is still detected at the end of the  
242 firing. The large peak shifts due to the thermal expansion of the compounds at high temperature  
243 makes it difficult to detect CaO. Nevertheless, calcium arsenate  $\text{Ca}_3(\text{AsO}_4)_2$  and possibly a very low  
244 presence of calcium cobalt pyroxene,  $\text{CaCoSi}_2\text{O}_6$ , are formed at about 775°C persisting up to 900°C  
245 and after cooling (**Figure 4a**).

246  
247 In summary, Arsenic is not completely lost and remains in the roasted material after firing.  
248  $\text{CoAs}_3$  is progressively transformed into an arsenic poorer compound during firing: from  $\text{CoAs}_3$  to  
249  $\text{CoAs}_2$  and finally to  $\text{CoAs}$  in agreement with some studies about decomposition/oxidation of  
250 skutterudite (Ertseva & Tsybulov, 2002; Mikhail et al., 1989; Wilson & Mikhail, 1989). Cobalt  
251 arsenate (phase A in **Figure 2**) is formed during heating as soon as skutterudite begins to  
252 decompose and is completely decomposed before 800 °C. Some of the cobalt reacts with the  
253 gangue and a small amount of a calcium cobalt silicate ( $\text{CaCoSi}_2\text{O}_6$ ) is formed. Calcium arsenate is  
254 formed when calcite decomposes and the CaO reacts with the arsenic oxide (**Figure 2**).

255  
256 The above results are in good agreement with Mikhail (Mikhail et al., 1989) study on  
257 skutterudite roasting which concluded that a complete removal of arsenic is not readily achievable  
258 under either oxidizing or inert conditions. Consequently, the presence of arsenic in the cobalt blue



259 glasses and glazes from the 16<sup>th</sup> century onwards is consistent with the use of *saffre* obtained by  
260 the process described by Kunckel (Kunckel, 1679).

261

#### 262 **4-COBALT AS A BY-PRODUCT OF SILVER SMELTING: LABORATORY TESTS**

263

264 The phases determined for the different mixtures of Table I at the *DP* maximum temperature  
265 (900°C) are reported in Table II. The transformations observed during the firing are detailed for  
266 each of the mixtures.

267

##### 268 *4.1 Cobalt arsenide ore, lead oxide, fluorite mixtures*

269 Lead oxide and fluorite are, according to Agricola after interpretation of Hoover (Georg  
270 Agricola, Agricola, Hoover & Hoover, 2011), the most important additions to the silver minerals in  
271 the smelting. They are the *fluxes of first and second order* respectively. In the smelting, the cobalt  
272 arsenides must have been a minor component of the smelt. For this reason, the mixture with the  
273 lowest cobalt ore content (m9) is reported with greater detail.

274

275 The diffractograms taken during the experiment are shown in **Figure 5**. PbO is in the form of  
276 massicot and litharge which are completely decomposed at 785°C and 827°C respectively.  
277 Skutterudite is decomposed at about 584°C and the arsenic released reacts with lead and fluorine  
278 producing  $Pb_5(AsO_4)_3F$  between 535 °C and 835 °C , (letter B in **Figure 5**),  $Pb_8As_2O_{13}$  between 560  
279 °C and 835 °C (letter C in **Figure 5**) and  $Pb_2OF_2$  between 567 °C and 785 °C (letter D in **Figure 5**).  
280 Calcium lead arsenate with the structure of hedyphane but with fluorine instead of chlorine,  
281  $(Ca,Pb)_5(AsO_4)_3F$ , is identified between 820 °C and 900°C. We have to mention that cobalt  
282 arsenates are not formed. Galena, PbS, (letter E in **Figure 5**) is formed by the reaction of lead with  
283 the sulphur released from cobalt ore between 535 °C and 852 °C. At the end of the firing only  
284 calcium lead arsenate  $(Ca,Pb)_5(AsO_4)_3F$  and fluorite are found (**Figure 4b**). The most representative  
285 diffractograms taken along the capillary at RT after firing are also shown in **Figure 6** Elongated  
286 crystals of calcium lead arsenate are seen over fluorite cubes by SEM (**Figure 7a**). The data  
287 indicates that lead reacts with fluorite and favours the decomposition of skutterudite promoting  
288 the formation of calcium lead and lead arsenates with fluorine and lead oxide with fluorine.

289

290 Finally, quartz reacts with PbO forming a glassy phase as is observed in the SEM image, **Figure**  
291 **7b**, and is also evident as a rising background in the diffraction patterns above 840°C (**Figure 5**).  
292 The blue particles with various shades seen in the capillaries correspond to a vitreous phase  
293 (**Figure S3**). Co is determined in the blue vitreous particles confirming the results of Wood and Hsu  
294 (2019).

295  
296 If a larger amount of cobalt ore is added to the mixture (m2), langisite and clinosafflorite are  
297 formed at intermediate temperatures (langisite appears in larger amounts than in m1) remaining  
298 in the final fired product. Consequently, cobalt arsenides are still present when lower amounts of  
299 lead oxide and fluorite are added. The colour of this mixture is dark blue (**Figure S3**).

300  
301 The presence of arsenate acicular crystals is often found in blue ceramic glazes after 1520 aD  
302 (among other: Hancock et al, 2000; Capelli, et al., 2002; Viti et al., 2003; Zucchiatti et al., 2006b;  
303 Tite 2009; Pradell et al., 2013; Van Pevenage et al., 2014; Colomban et al., 2017, 2018, 2020; de  
304 Viguerie et al., 2019). In particular the presence of lead rich KNaPb arsenates ( $\text{NaKPb}_8(\text{AsO}_4)_6$ ) with  
305 apatite structure have been determined by SR-XRD (Pradell et al., 2013). Van Pevenage et al.  
306 (2014) found a lead arsenate similar to mimetite ( $\text{Pb}_5(\text{AsO}_4)_3\text{Cl}$ ) in the pigments of the ruan-cai  
307 blue colour Chinese porcelain dating from the 18th century. Colomban et al. (2018) detected lead  
308 arsenates by Raman of blue-decorated early soft-paste porcelain after 1750 and lead arsenate  
309 apatite phase of the type  $\text{Na}_{1-x-y}\text{K}_x\text{Ca}_y\text{Pb}_4(\text{AsO}_4)_3$  in 17th–18th century enamelled French watches.  
310 Although the presence of acicular arsenate crystals is often described, the phases have been rarely  
311 unambiguously identified.

312  
313 In this study, crystalites of  $(\text{Ca,Pb})_5(\text{AsO}_4)_3\text{F}$  have been detected for the first time. We added  
314 fluorite, and the phase formed is equivalent to hedyphane ( $\text{Ca}_2\text{Pb}_3(\text{AsO}_4)_3\text{Cl}$ ) but with F instead of  
315 Cl. Hedyphane has an apatite like structure and contains Cl but it may also contain OH  
316 (hydroxilhedyphane) and F (fluorhedyphane) (Pesaro, et al. 2010).

317  
318 In fact similar calcium lead arsenate crystallites were also found in Catalan Blue wares with the  
319 following composition ( $\text{Ca}_{2.74}\text{Pb}_{2.26}\text{P}_{0.39}\text{As}_{2.61}\text{O}_{12}\text{Cl}_{0.19}$ ) determined by microprobe (**Figure 8a and**  
320 **8b**). The Rietveld refinement of this structure with Fullprof software (Rodríguez-Carvajal, 1993)

321 using as starting model the described structure for hedyphane (Rouse et al., 1984) shows an  
322 excellent match (**Figure 8c**) with cell parameters  $a=b=9.9320(3)$  Å and  $c=7.1001(2)$  Å,  $V=606.56(3)$   
323 Å<sup>3</sup>. This verifies the formation of this type of calcium lead arsenates also in historical glazes.

324  
325 Although the amount of arsenic present in the glazes is normally very low, the precipitation of  
326 lead arsenates and in particular the arsenates with hedyphane structure is expected to happen  
327 and their presence is a marker of the use of cobalt arsenide ore.

328  
329 When the mixture m9 is fired at 1200°C in *SP* mode (definitely out of reach for 15<sup>th</sup> and 16<sup>th</sup>  
330 century smelters and also for SR-XRD air blower used) only calcium arsenate crystals are found  
331 (hexagonal prismatic and acicular) (**Figure 7c**) together with aggregates of tiny crystals rich in  
332 cobalt, iron and nickel (**Figure 7d**). Flat, approximately rectangular, calcium aluminosilicate  
333 crystallites (anorthite type) resulting from the reaction with the alumina crucible were also formed  
334 at this high temperature.

335  
336 *4.2 Cobalt arsenide ore, lead oxide, fluorite, quartz Mixtures*

337 From the *DP* analysis of mixture m4 we observe that the addition of quartz favours the  
338 development of the liquid phase producing a more vitrified product (lead silicate vitreous phase).  
339 After firing at 900°C only very little langisite, (Co,Ni)As, lead fluoride arsenate  $Pb_5(AsO_4)_3F$  and  
340 fluorhedyphane  $(Ca,Pb)_5(AsO_4)_3F$  are present, along with quartz, cristobalite and fluorite. With a  
341 lower amount of the cobalt ore (m11) the material obtained is even more vitrified and the cobalt  
342 arsenides are residual (**Figure 4b and Figure 9**). The vitreous phase appears blue in the capillaries  
343 (**Figure S3**) which are related to the vitreous phase which incorporates the cobalt (**Figure S4**).

344  
345 *4.3 Cobalt arsenide ore, lead oxide, calcite, kaolinite*

346 Fluorite was added in the previous mixtures as a flux in silver smelting because it was  
347 mentioned in the Agricola text as *stones which fuse easily by fire of the second order*. But, fluor is  
348 not normally determined in the analyses of glazes and glass. For this reason, calcite has been  
349 added instead of fluorite. A mixture incorporating calcite and  $Pb_3O_4$  instead of  $PbO$  (m16, Table I)  
350 have been produced to explore the effect that different sources of Pb and Ca had in the final  
351 product. Moreover, some kaolinite, which was present in the kiln walls, was also added to check  
352 its effect in the final slag obtained.

353

354 The SR-XRD patterns (**Figure 10** and **Figure 4c**) show that  $Pb_3O_4$  and kaolinite disappear at  
355 591°C and 676°C respectively, while skutterudite and calcite decompose completely at 692°C and  
356 900°C. Kaolinite ( $Al_2Si_2O_5(OH)_4$ ) promotes the formation of lead feldspars ( $PbAl_2Si_2O_8$ ). Both the  
357 stable monoclinic and the metastable hexagonal lead feldspar are formed during the firing at  
358 about 700°C, and the monoclinic phase increases from 845°C to 900°C. Finally, calcium lead  
359 arsenates with hedyphane structure but incorporating OH,  $(Ca,Pb)_5(AsO_4)_3OH$   
360 (Hydroxylhedyphane) are formed at about 700°C increasing at 845°C. A glassy phase is also formed  
361 (**Figure S4b**) but in lower amounts than in the mixtures m4 and m11. The SEM observation  
362 indicates that the cobalt is concentrated in the glassy particles, as in the previous cases.

363

## 364 5- DISCUSSION

365

366 Our laboratory tests have proved that roasting a rich cobalt arsenide ore at high temperature  
367 or even for a long time is unable to remove completely the arsenic from the ore. The typical  
368 composition of historical blue glazes after 1520 is perfectly compatible with the material obtained  
369 roasting of minerals from the cobalt arsenides deposits of the Erzgebirge area (Weber, 1986), to  
370 produce *saffre*, as described by Kunckel (Kunckel, 1679).

371

372 Our replication of the processes described by Agricola gave rise to the formation of a lead rich  
373 silica glassy phase which incorporates cobalt in variable amounts together with calcium and lead  
374 arsenates of various compositions. We have also found that the amount and composition of the  
375 glassy phase depends on the amount of quartz and lead oxide and fluorite added. Adding a larger  
376 amount of quartz and fluxes a most extensive glassy phase is obtained and less crystalline  
377 compounds (calcium lead arsenates) are produced. As the physical separation of the different  
378 phases does not appear possible, the question is then reduced to the possible commercialization  
379 and use of the material obtained by this process in the production of cobalt blue glazes.  
380 Considering that the glassy phase would integrate into the glaze, part of the arsenic still present  
381 would be removed in the glaze firing and the remaining arsenic would either dissolve or  
382 recrystallise into calcium lead arsenate, the use of the subproduct obtained to tinge lead glazes  
383 could not be discarded. This could account for the variable content of arsenic shown by the  
384 historical glazes. However, as fluor has not been reported in the historical glazes, either fluorite

385 was added in low amounts or another flux was added instead. We should mention that the  
386 presence of fluorite has been reported in the white but also blue Chinese cloisonné enamels  
387 (Colomban et al., 2020). The use of fluorite is not clear in Agricola's description of the process and  
388 other fluxes could have been added instead. In fact, the processing described by Agricola and  
389 replicated in this study produces, among other compounds, a cobalt blue glassy product not very  
390 different from *smalt*, as *smalt* is also a cobalt blue glass obtained adding quartz and a flux, in this  
391 case potash.

392

393 The study has also provided direct evidence of the crystallisation of an hedyphane type of  
394 calcium lead arsenates, incorporating Cl, F or OH. A phase which has been found in historical  
395 glazes, but never properly identified until now.

396

397 Our results indicate that an arsenic free cobalt compound could not have been produced by a  
398 higher temperature treatment of skutterudite or during the smelting of silver as described by  
399 Agricola (Agricola, Hoover & Hoover, 2011). Therefore, other sources of cobalt must be considered  
400 to explain the appearance, between the beginning of the 15<sup>th</sup> century and the third decade of the  
401 16<sup>th</sup> century of the CoNi with trace amounts of As pigment used to colour blue glasses and glazes.

402

403 Since the coeval literature describes blue pigments as coming from *la Magna* (Cennini, 1400)  
404 the minerals of the Erzgebirge must again be considered. Agricola (Agricola, 1530) gives account  
405 of the existence of different cobalt minerals but with the same *properties*, saying, in particular,  
406 that all were corrosive because of their As content. Andrews (Andrews, 1962) reports that "*the*  
407 *principal deposits of the Erzgebirge, consisting of smaltite, erythrite, linnaeite and asbolane in*  
408 *association with barites, silver and bismuth, occur in contact-metamorphosed slates underlain by*  
409 *granites...*".

410

411 An As free Co from *la Magna* could have come from the processing of linnaeite ( $\text{Co}^{2+}\text{Co}^{3+}_2\text{S}_4$ ) or  
412 asbolane  $((\text{Co},\text{Ni})_{1-y}(\text{Mn}^{4+}\text{O}_2)_{2-x}(\text{OH})_{2-2y+2x}\cdot n(\text{H}_2\text{O}))$  a mixture of hydrated Co and Mn oxides). The  
413 PIXE analysis of blue glazes of the *della Robbia* production, whenever As is below PIXE detection  
414 limits, do not show sufficient Mn content to support the origin of the *saffre* from asbolane that  
415 contains more Mn (65-96%) than Co (35-4%) (Andrews R.W, 1962). In the group of *della Robbia*  
416 sculptures dated before 1520, we found a MnO/CoO ratio always below 0.20 except when

417 manganese was deliberately added to make the blue turn violet or when a black coloured glaze  
418 diffused into the blue glaze during firing.

419

420 As concerns linnaeite, there are significant coincidences between what is reported above for  
421 the *della Robbia* glazes (Zucchiatti et al., 2006a) and for the 9<sup>th</sup> century Islamic Samarra faiences  
422 (Kleinman, 1990). Kleinmann's morphological analysis reveals the presence of pigment remnants  
423 in three phases aggregates: a granulated nucleus, surrounded by silicate crystals in a vitreous  
424 matrix. The granulated nuclei were identified as Co-Fe-Ni spinels with an extremely variable  
425 composition (Co 13.90-47.69%; Fe 9.51-82.13%; Ni 1.01-59.15%). The same kind of structure will  
426 reappear (Kleinmann, 1986; Kleinmann, 1987) in medieval Persian faiences. Linnaeite would fit,  
427 according to Kleinmann, with the description (Allan, 1973) of a stone "... like white silver shining  
428 in a sheath of hard black stone". Will fit also with the morphology observed in the *della Robbia*  
429 blue glazes prior to 1520 and, finally, with the quite variable relation between the characterizing  
430 elements Co-Fe-Ni, detected by PIXE in the As free glazes. Roasted linnaeite would fit much better  
431 than arsenates or sulpho-arsenates as the origin of the specific Co-Ni group. It might be that the  
432 *della Robbia* used, before the advent of the *saffre*, the same pigment that was utilized in the blue  
433 and white Chinese porcelain of the early Ming period (1368-1424). This was characterized by a  
434 very high Fe/Mn ratio (Wen et al., 2007) that we find as well in the analyses of the *della Robbia*  
435 glazes ( $Fe_2O_3/MnO > 15$ ). The pigment is very similar to the one found in Middle Eastern ceramics  
436 from the 9<sup>th</sup> century onwards and could correspond to the so-called *Sumali* blue probably  
437 exported, from Iran, both to the Far East and Europe.

## 438 **7-CONCLUSIONS**

439

440 We performed laboratory tests to investigate the production of cobalt materials in blue glazed  
441 ceramics from the Renaissance. The previous analyses of ancient glass and glaze put in evidence  
442 a change of the cobalt material at the edge between the 15<sup>th</sup> and 16<sup>th</sup> century. The replication of  
443 the roasting process of a natural cobalt arsenide ore has shown that a complete removal of arsenic  
444 is not obtained, which explains the presence of arsenic in the cobalt blue glasses and glazes from  
445 the 16<sup>th</sup> century onwards. Our results fit very closely with the description of the process done in  
446 historical texts and with the beginning of trade of a new commercial material, called *saffre*, from  
447 the rich cobalt arsenides deposits of the Erzgebirge area.

448

449 Assuming that cobalt could have been a slag of the massive silver smelting in the Erzgebirge  
450 area and following the description that Agricola gives of the silver mining and smelting, we have  
451 produced various mineral mixtures and followed their transformation, mimicking the smelting  
452 process. Our replication of the processes described by Agricola gave rise to the formation of a lead  
453 rich glassy phase which incorporates cobalt in variable amounts together with lead arsenates  
454 ( $\text{Pb}_5(\text{AsO}_4)_3\text{F}$ ,  $\text{Pb}_8\text{As}_2\text{O}_{13}$ ) and calcium lead arsenates ( $(\text{Ca,Pb})_5(\text{AsO}_4)_3(\text{F,Cl,OH})$ ) with an hedyphane  
455 structure, while cobalt is incorporated into a glassy matrix. When kaolinite is added, lead feldspars  
456 are also formed. Therefore, the separation of the cobalt from arsenic is accomplished. However,  
457 as the physical separation of the cobalt glassy phase from the other crystalline compounds does  
458 not appear possible, the question is then reduced to the possible commercialization and use of  
459 the material obtained by this process in the production of cobalt blue glazes. Although the use of  
460 this slag as a cobalt pigment to tinge lead glazes cannot be discarded, the material obtained is not  
461 arsenic free and therefore, it can hardly account for the arsenic free material like the one used by  
462 the *della Robbia* and other before 1515-1520.

463

464 In addition, it is not straightforward to justify a consistent production of cobalt materials with  
465 the much lower abundance of linnaeite in the Erzgebirge (Seifert & Sandmann, 2006). It is worth  
466 observing that the revision of available data puts in evidence some compositional similarity  
467 between the *della Robbia* sculptures, the Near East pottery and the Chinese blue and white  
468 porcelain. The similarity might be explained by the common use of arsenic free cobalt materials  
469 produced, for example, from linnaeite in the Qamsar mines in Iran and traded towards the  
470 Mediterranean basin and China before the massive introduction on the market of the German  
471 *saffre*. The processing of linnaeite definitely deserves specific studies, both dynamical and  
472 microscopic, as we did so far for the cobalt arsenide ore.

473

#### 474 **ACKNOWLEDGMENTS**

475 One of us (A.Z.) is pleased to acknowledge the support of Istituto Nazionale di Fisica Nucleare  
476 of Italy and Universidad Autónoma de Madrid at the time he performed part of this work being a  
477 member of their respective staff. We are indebted to the Centre de Recherche et Restauration des  
478 Musées de France. Experiments were performed at BL04 MSPD Beamline at ALBA synchrotron  
479 Facility with the collaboration of Alba Staff (Ref. 2018092994, 2018022748, 2015091398) for  
480 financial support during part of this work. We are indebted to professors Badra and Haddad of

481 the Moulay Ismail University of Meknes (Morocco) for providing us with the cobalt ore. J.M. and  
482 T.P. are grateful to the project PID2019-105823RB-I00 funded by the Ministerio de Ciencia e  
483 Innovación (Spain) and TP is grateful to Generalitat de Catalunya grant 2017SGR-0042.

484



485

## References

486

Agricola, G. (1530). *Bermannus Sive De Re Metallica Dialogus*. available at the Biblioteca Nazionale Braidense, Milano, Italy.

487

488

Agricola, Georg, Agricola, G., Hoover, H. & Hoover, L. H. (2011). Georgius Agricola De re metallica, tr. from the 1st Latin ed. of 1556, with biographical introduction, annotations and appendices upon the development of mining methods, metallurgical processes, geology, mineralogy & mining law, from t. In *Georgius Agricola De re metallica, tr. from the 1st Latin ed. of 1556, with biographical introduction, annotations and appendices upon the development of mining methods, metallurgical processes, geology, mineralogy & mining law, from the earliest times to the 16th century*.

489

490

491

492

493

494

495

<https://doi.org/10.5962/bhl.title.30118>

496

Ahmed AH, Arai S, Ikenne M (2009a) Mineralogy and paragenesis of the Co-Ni arsenide ores of Bou Azzer, Anti-Atlas, Morocco. *Econ Geol* 104:249–266

497

498

Allan, J. W. (1973). Abū'l-Qāsim's Treatise on Ceramics. *Iran*.

499

<https://doi.org/10.2307/4300488>

500

Andrews R.W. (1962). Cobalt. In *Overseas Geological Surveys. Minerals resources Division. Her Majesty's stationery office*.

501

502

Bajnóczi, B., Nagy, G., Tóth, M., Ringer, I. & Ridovics, A. (2014): Archaeometric characterization of 17th-century tin-glazed Anabaptist (Hutterite) faience artefacts from North-East-Hungary. *Journal of Archaeological Science*, 45, 1-14.

503

504

505

<https://doi.org/10.1016/j.jas.2014.01.030>

506

Calligaro, T., Dran, J. C., Ioannidou, E., Moignard, B., Pichon, L., & Salomon, J. (2000). Development of an external beam nuclear microprobe on the aglae facility of the Louvre museum. *Nuclear Instruments and Methods in Physics Research, Section B: Beam Interactions with Materials and Atoms*, 161, 328–333. [https://doi.org/10.1016/S0168-583X\(99\)00899-X](https://doi.org/10.1016/S0168-583X(99)00899-X)

507

508

509

510

511

Capelli, C. & Riccardi, M. P. (2002): Il contributo delle analisi petrografiche allo studio dei rivestimenti di ceramiche in blu: alcuni esempi. Atti XXXV convegno internazionale della ceramica. Ceramica in blu, diffusione e utilizzazione del blu nella ceramica. Savona, 31 maggio – 1 giugno. Centro Ligure per la storia della ceramica, Albisola, 19-28.

512

513

514

515

Cennini, C. (1400). *Il libro dell'arte, o Trattato della pittura* (1859 a cura di Gaetano e Carlo Milanesi, Le Monnier, Firenze (ed.)).

516

517

Colomban, P., Arberet, L., & Kirmizi, B. (2017). On-site Raman analysis of 17th and 18th century Limoges enamels: Implications on the European cobalt sources and the technological relationship between Limoges and Chinese enamels. *Ceramics International*. <https://doi.org/10.1016/j.ceramint.2017.05.040>

518

519

520

521

Colomban, P., Maggetti, M., & d'Albis, A. (2018). Non-invasive Raman identification of crystalline and glassy phases in a 1781 Sèvres Royal Factory soft paste porcelain plate.

522

- 523 *Journal of the European Ceramic Society.*  
524 <https://doi.org/10.1016/j.jeurceramsoc.2018.07.001>
- 525 Colomban, P., Kırmızı, B., Gougeon, C., Gironda, M. & Cardinal, C. (2020). Pigments and glassy  
526 matrix of the 17th-18th century enamelled French watches: a non invasive on-site  
527 Raman and pXRF study. *Journal of Cultural Heritage*, 44[1-14].  
528 <https://doi.org/10.1016/j.culher.2020.02.001>
- 529 de Viguerie, L., Robador, M. D., Castaing, J., Perez-Rodriguez, J. L., Walter, P., & Bouquillon, A.  
530 (2019). Technological evolution of ceramic glazes in the renaissance: In situ analysis of  
531 tiles in the Alcazar (Seville, Spain). *Journal of the American Ceramic Society.*  
532 <https://doi.org/10.1111/jace.15955>
- 533 Ertseva, L. N. & Tsymbulov, L. B. (2002). On transformations of iron, nickel, and cobalt  
534 arsenides and sulfoarsenides under thermal treatment in various media. In *Russian*  
535 *Journal of Applied Chemistry.* <https://doi.org/10.1023/A:1022290609934>
- 536 Fauth, F., Peral, I., Popescu, C., & Knapp, M. (2013). The new material science powder  
537 diffraction beamline at ALBA synchrotron. *Powder Diffraction.*  
538 <https://doi.org/10.1017/S0885715613000900>
- 539 Gratuze, B., Pactat, I., & Schibille, N. (2018). Changes in the signature of cobalt colorants in  
540 late antique and early Islamic glass production. *Minerals.*  
541 <https://doi.org/10.3390/min8060225>
- 542 Gratuze, B., Soulier, I., Barrandon, J. N., & Roy, D. (1992). De l'origine du cobalt dans les  
543 verres. *Revue d'Archéométrie.* <https://doi.org/10.3406/arsci.1992.895>
- 544 Gratuze, B., Soulier, I., Blet, M., & Vallauri, L. (1996). De l'origine du cobalt : du verre à la  
545 céramique. *Revue d'Archéométrie.* <https://doi.org/10.3406/arsci.1996.939>
- 546 Hancock, R.G.V., McKenzie, J., Aufretier, S.; Karklins, K., Kapches, M., Sempowski, M.,  
547 Moreau, J.J., Kenyon, I. (2000). Non-destructive analysis of European cobalt blue trade  
548 beds. *Radioanal. Nucl. Chemistry*, 244 [3], 567-573.
- 549 Johansson, S. A. E., Campbell, J. L., Malmqvist, K., & Winefordner, J. (1995). Particle-Induced  
550 X-Ray Emission Spectrometry (PIXE) Edited by Sven A. E. Johansson (Sweden), John L.  
551 Campbell (Canada), and Klas G. Malmqvist (Sweden). Wiley & Sons: New York. 1995. xxiii  
552 + 451 pp. \$79.95. ISBN 0-471-58944-6. In *Journal of the American Chemical Society.*  
553 <https://doi.org/10.1021/ja955314e>
- 554 Kleinman, B. (1990). Cobalt-pigments in the Early Islamic blue glazes and the reconstruction  
555 of the way of their manufacture. In *Archaeometry 90: Proceedings of the 27th*  
556 *International Symposium on Archaeometry.*
- 557 Kleinmann, B. (1986). History and development of early Islamic pottery glazes. In *Proceedings*  
558 *of the twenty-fourth International Archaeometry Symposium.*

- 559 Kleinmann, Barbara. (1987). Technological studies of Medieval and later Persian faience:  
560 possible successors to the faience of antiquity. In *Early vitreous materials*.
- 561 Kunckel, J. (1679). *Ars vitraria experimentalis, Oder Vollkommene Glasmacher-Kunft*  
562 *Lehrende*, Franckfurt und Leipzig
- 563 Matin, M., & Pollard, M. (2015). Historical accounts of cobalt ore processing from the Kashan  
564 Mine, Iran. In *Iran*. <https://doi.org/10.1080/05786967.2015.11834755>
- 565 Melzer, C. (1684). *Berglaufftige Beschreibung der Stadt Schneeberg*.
- 566 Mikhail, S. A., Turcotte, A. M., & Bowman, W. S. (1989). A study of the decomposition of  
567 higher cobalt arsenides by thermal analysis. *Thermochemica Acta*.  
568 [https://doi.org/10.1016/0040-6031\(89\)85442-5](https://doi.org/10.1016/0040-6031(89)85442-5)
- 569 Mühlethaler, B., Thissen, J. (1969). *Smalt. Stud. Conserv.*, 14, 47-61
- 570 Pappalardo, G., Costa, E., Marchetta, C., Pappalardo, L., Romano, F. P., Zucchiatti, A., Prati, P.,  
571 Mandò, P. A., Migliori, A., Palombo, L., & Vaccari, M. G. (2004). Non-destructive  
572 characterization of Della Robbia sculptures at the Bargello museum in Florence by the  
573 combined use of PIXE and XRF portable systems. *Journal of Cultural Heritage*.  
574 <https://doi.org/10.1016/j.culher.2003.08.002>
- 575 Pérez-Arantegui, J., Resano, M., García-Ruiz, E., Vanhaecke, F., Roldán, C., Ferrero, J., & Coll,  
576 J. (2008). Characterization of cobalt pigments found in traditional Valencian ceramics by  
577 means of laser ablation-inductively coupled plasma mass spectrometry and portable X-  
578 ray fluorescence spectrometry. *Talanta*, 74(5), 1271–1280.  
579 <https://doi.org/10.1016/j.talanta.2007.08.044>
- 580 Pesaro, M., Kampf, A.R., Ferrari, C., Pekov, I.V., Rakovans, J., White, T.J. (2010). Nomenclature  
581 of the apatite supergroup minerals. *Eur. J. Mineral.*, 22, 163–179
- 582 Porter, Y. (1997). Origines et diffusion du cobalt utilisé en céramique à l'époque médiévale.  
583 Etude préliminaire. In *La céramique médiévale en Méditerranée. Actes du VI<sup>e</sup> congrès*  
584 *international*. (pp. 505–512).
- 585 Pradell, T., Molina, G., Molera, J., Pla, J., & Labrador, A. (2013). The use of micro-XRD for the  
586 study of glaze color decorations. *Applied Physics A: Materials Science and Processing*,  
587 111(1), 121–127. <https://doi.org/10.1007/s00339-012-7445-x>
- 588 Prati P. and Massabò D. (2019). *private communication*.
- 589 Rodríguez-Carvajal, J. (1993). Recent advances in magnetic structure determination by  
590 neutron powder diffraction. *Physica B: Physics of Condensed Matter*.  
591 [https://doi.org/10.1016/0921-4526\(93\)90108-l](https://doi.org/10.1016/0921-4526(93)90108-l)
- 592

- 593 Roldán, Clodoaldo, Coll, J., & Ferrero, J. (2006). EDXRF analysis of blue pigments used  
594 in Valencian ceramics from the 14th century to modern times. *Journal of Cultural*  
595 *Heritage*. <https://doi.org/10.1016/j.culher.2006.02.003>
- 596 Rouse, R. C., Dunn, P. J., & Peacor, D. R. (1984). Hedyphane from Franklin, New Jersey and  
597 Langban, Sweden: cation ordering in an arsenate apatite. *American Mineralogist*.
- 598 Seifert, T., & Sandmann, D. (2006). Mineralogy and geochemistry of indium-bearing  
599 polymetallic vein-type deposits: Implications for host minerals from the Freiberg district  
600 Eastern Erzgebirge, Germany. *Ore Geology Reviews*.  
601 <https://doi.org/10.1016/j.oregeorev.2005.04.005>
- 602 Soulier, I., Gratuze, B., & Barrandon, J.-N. (1996). The origin of cobalt blue pigments in French  
603 glass. In *Archaeometry 94: Proceedings of the 29th International Symposium on*  
604 *Archaeometry*.
- 605 Tite (2009) The production technology of Italian maiolica: a reassessment. *Journal of*  
606 *Archaeological Science*, 36, 2065-2080. <https://doi.org/10.1016/j.jas.2009.07.006>
- 607 Van Pevenage, J., Lauwers, D., Herremans, D., Verhaeven, E., Vekemans, B, De Clercq, W.,  
608 Vincze, L., Moensa L. and Vandenabeele, P. (2014). A combined spectroscopic study on  
609 Chinese porcelain containing ruan-cai colours. *Anal. Methods*, 2014, 6, 387
- 610 Viti, C., Borgia, I., Brunetti, B., Sgamellotti, A., & Mellini, M. (2003). Microtexture and  
611 microchemistry of glaze and pigments in Italian Renaissance pottery from Gubbio and  
612 Deruta. *Journal of Cultural Heritage*. [https://doi.org/10.1016/S1296-2074\(03\)00046-3](https://doi.org/10.1016/S1296-2074(03)00046-3)
- 613 Weber W. (1986). Der Freiburger Bergbau. *Lapis Mineralien Magazin*, 11, 13–27.
- 614 Wen, R., Wang, C. S., Mao, Z. W., Huang, Y. Y., & Pollard, A. M. (2007). The chemical  
615 composition of blue pigment on Chinese blue-and-white porcelain of the Yuan and Ming  
616 dynasties (AD 1271-1644). *Archaeometry*. [https://doi.org/10.1111/j.1475-](https://doi.org/10.1111/j.1475-4754.2007.00290.x)  
617 [4754.2007.00290.x](https://doi.org/10.1111/j.1475-4754.2007.00290.x)
- 618 Wilson, L. J., & Mikhail, S. A. (1989). Investigation of the oxidation by thermal analysis of  
619 skutterudite. *Thermochimica Acta*, 156(1), 107–115.
- 620 Wood, J.R. and Hsu, Y.T. 2019 An Archaeometallurgical Explanation for the Disappearance of  
621 Egyptian and Near Eastern Cobalt-Blue Glass at the end of the Late Bronze Age, *Internet*  
622 *Archaeology* 52. <https://doi.org/10.11141/ia.52.3>
- 623 Zucchiatti, A., Bouquillon, A., Katona, I., & D’Alessandro, A. (2006a). The “della Robbia blue”:  
624 A case study for the use of cobalt pigments in ceramics during the Italian Renaissance.  
625 *Archaeometry*. <https://doi.org/10.1111/j.1475-4754.2006.00247.x>
- 626 Zucchiatti, A., Bouquillon, A., Katona, I., & D’Alessandro, A. (2006b). The “della Robbia blue”:  
627 A case study for the use of cobalt pigments in ceramics during the Italian Renaissance.  
628 *Archaeometry*, 48(1), 131–152. <https://doi.org/10.1111/j.1475-4754.2006.00247.x>

629 Zucchiatti, A., Bouquillon, A., Moignard, B., Salomon, J., & Gaborit, J. R. (2000). Study of  
630 Italian Renaissance sculptures using an external beam nuclear microprobe. *Nuclear*  
631 *Instruments and Methods in Physics Research*, Section B: Beam Interactions with  
632 Materials and Atoms. [https://doi.org/10.1016/S0168-583X\(99\)00905-2](https://doi.org/10.1016/S0168-583X(99)00905-2)

633

634

635 **FIGURE CAPTIONS**

636  
637 **Figure 1** . The As and Co weight percent in the cobalt arsenide ore (mixture m1 in Table I) and at  
638 different roasting temperatures determined by PIXE. Quantitative analysis was performed on  
639 millimetric scanned areas. The percent errors are around 2% and do not exceed the marker size.

640  
641 **Figure 2**. Diffractogram evolution of cobalt arsenide ore (mixture m1 in Table I) from room  
642 temperature (top pattern) to the maximum temperature of 900 °C (red pattern) and cooling to  
643 room temperature (bottom pattern). The green diffractogram corresponds to 573 °C ( $\alpha$ -quartz  
644 to  $\beta$ -quartz transition).

645  
646 **Figure 3**. SR-XRD patterns corresponding to the cobalt arsenide ore (mixture m1 in Table I). (a)  
647 before heating, (b) white zone of capillary (c) dark zone of capillary, (d) zone of maximum  
648 heating collected at RT after cooling.

649  
650 **Figure 4**. Thermal stability ranges of phases of m1, m9 and m16.

651  
652 **Figure 5**. Diffractogram evolution of mixture m9 (Table I) from room temperature (top pattern)  
653 to the maximum temperature of 900 °C (red pattern) and cooling to room temperature (bottom  
654 pattern). The mixture components at RT, are identified by the symbols in the legend. The phases  
655 formed during the thermal treatment are indicated by the letter B to E.

656  
657 **Figure 6**. SR-XRD patterns corresponding to the mixture m9 (Table I). (a) before heating, (b)  
658 external zone of capillary (c) middle zone of capillary, (d) near maximum temperature of capillary  
659 (e) zone of maximum heating collected at RT after cooling.

660  
661 **Figure 7**. SEM images of mixture m9 fired at 900°C (DP) (a) and (b) and 1200°C (c) and (d) (SP).  
662 (a) Lead arsenate tiny crystals (2) grown over cubes of fluorite (1).  
663 (b) Fluorite crystals (1) surrounded by lead rich vitreous phase (2).  
664 (c) Calcium arsenate crystals (1) and calcium aluminosilicate crystallites (anorthite type) (2).  
665 (d) Calcium arsenates crystals (1) and aggregates of tiny crystals rich in cobalt, iron and nickel (2)

666

667

668

669

670

671

672

**Figure 8.** Blue decorated Catalan glaze from 18th century (SBG17). (a) Thin section of glaze. The blue decoration was applied overglaze. The Ca-Pb arsenates acicular crystals  $((\text{Ca,Pb})_5(\text{AsO}_4)_3\text{Cl})$  are formed in the contact between tin lead glaze and blue decoration layer. B) SEM BSE image of Ca-Pb arsenates (white colour) and lead feldspars (grey colour). C) Rietveld refinement of the Ca-Pb arsenate apatite-like structure.

673

674

675

676

**Figure 9.** Diffractogram evolution of mixture m11 (Table I) from room temperature (top pattern) to the maximum temperature of 900 °C (red pattern). The green diffractogram corresponds to 573 °C (quartz alpha to quartz beta transition).

677

678

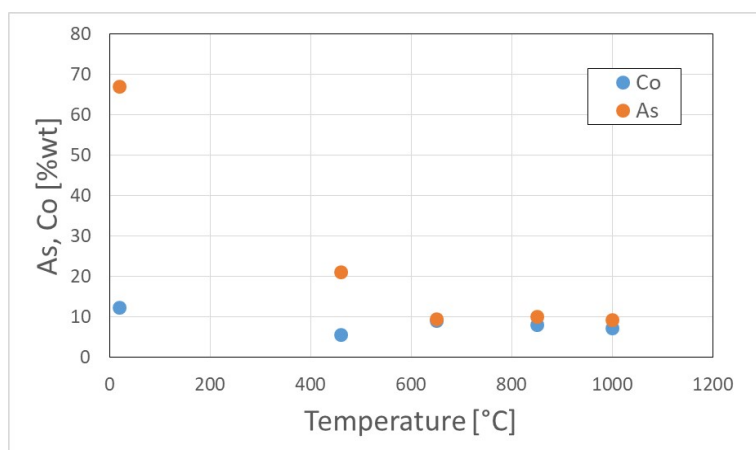
679

680

681

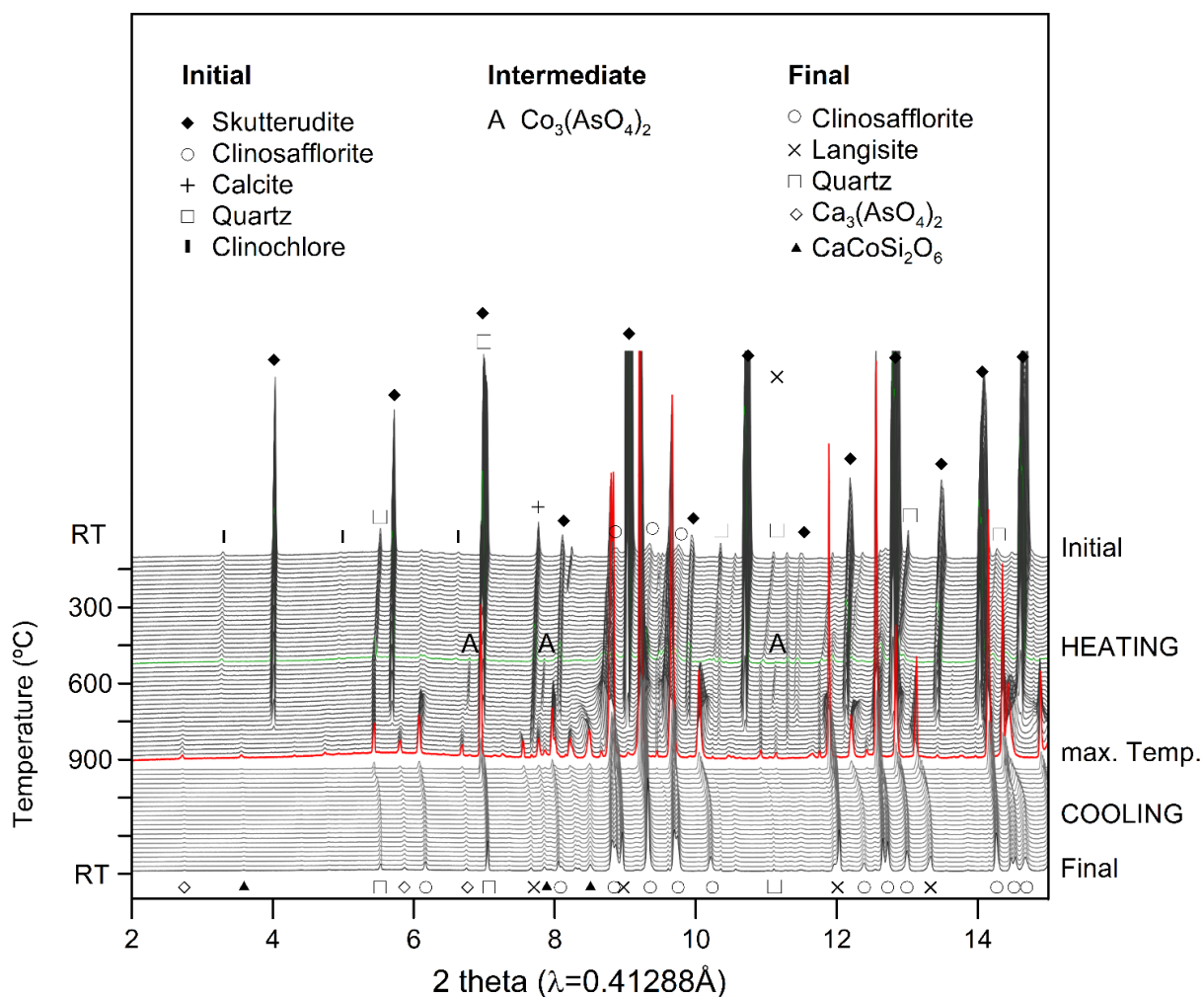
**Figure 10.** Diffractogram evolution of mixture m16 (Table I) from room temperature (top pattern) to the maximum temperature of 900 °C (red pattern). The green diffractogram corresponds to 573 °C (quartz alpha to quartz beta transition).

682 Figures  
 683



684  
 685  
 686  
 687  
 688  
 689  
 690  
 691

Fig.1. Co and As content (wt%) in the raw cobalt ore and at different roasting temperatures determined by PIXE.

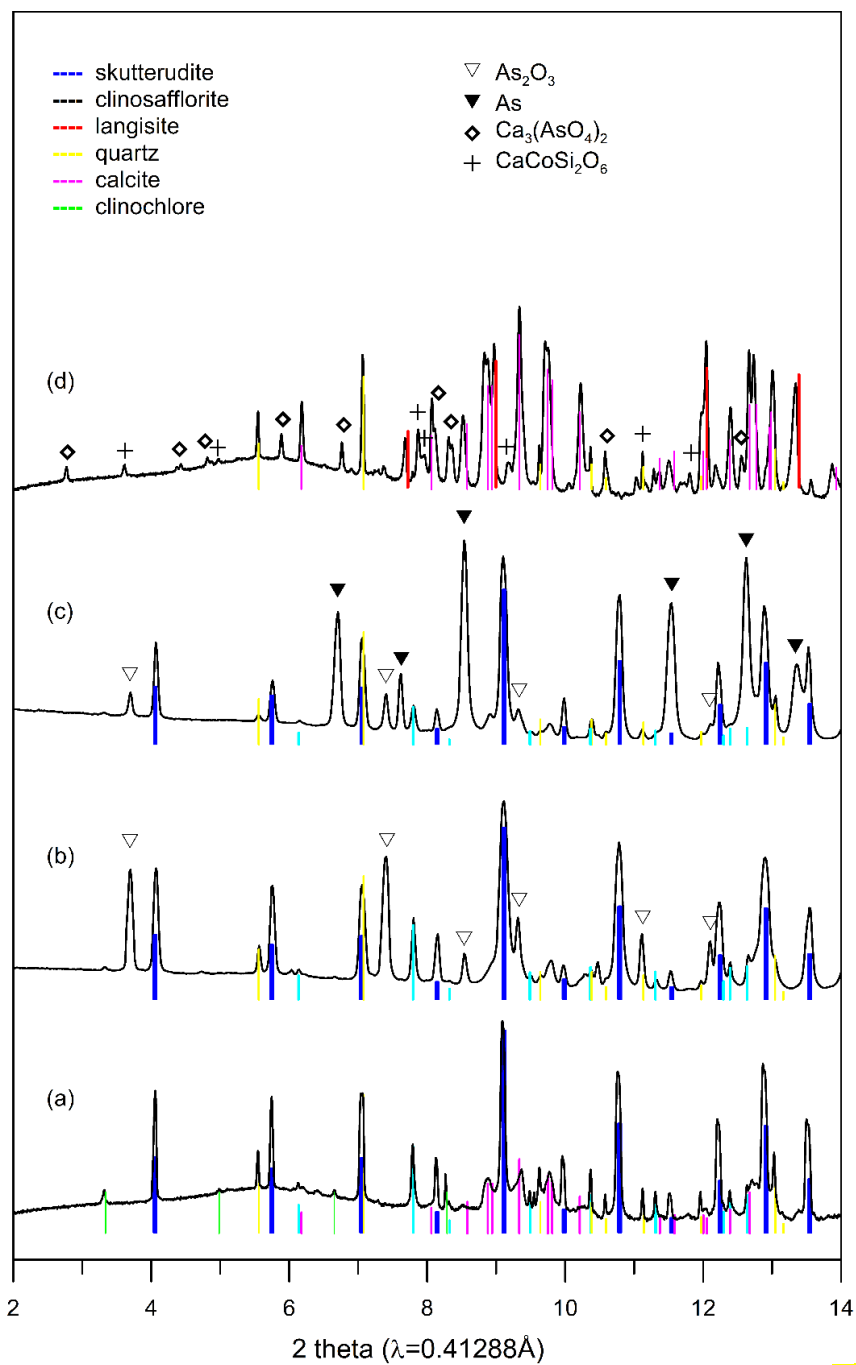


692  
 693  
 694

Figure 2. Diffractogram evolution of cobalt arsenide ore (mixture m1 in table I) from room temperature (top pattern) to the maximum temperature of 900 °C (red pattern) and cooling to room

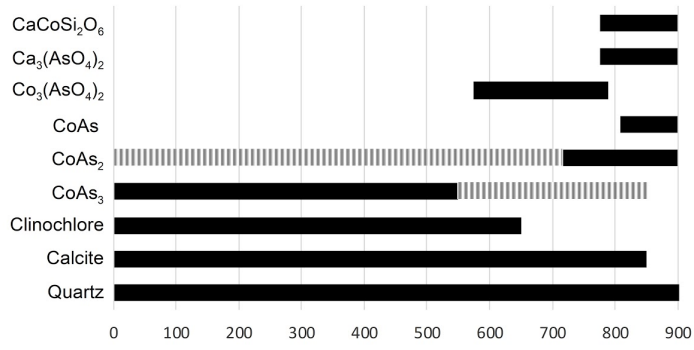


695 temperature (bottom pattern). Green diffractogram corresponds to 573 °C ( $\alpha$ -quartz to  $\beta$ -quartz  
696 transition).  
697

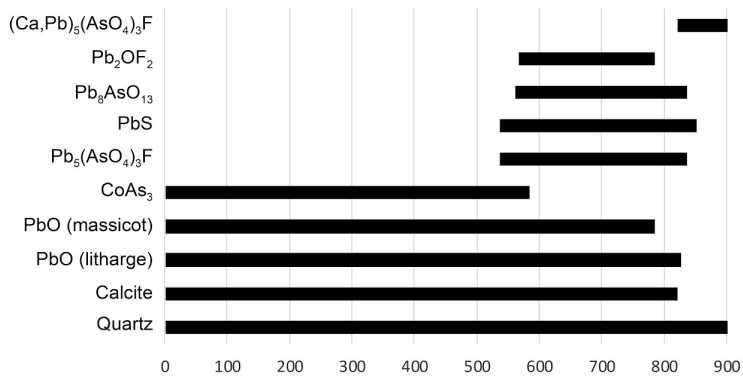


698  
 699 **Figure 3.** SR-XRD patterns corresponding to the cobalt arsenide ore (mixture m1 in table I). (a)  
 700 before heating, (b) white zone of capillary (c) dark zone of capillary, (d) zone of maximum heating  
 701 collected at RT after cooling.

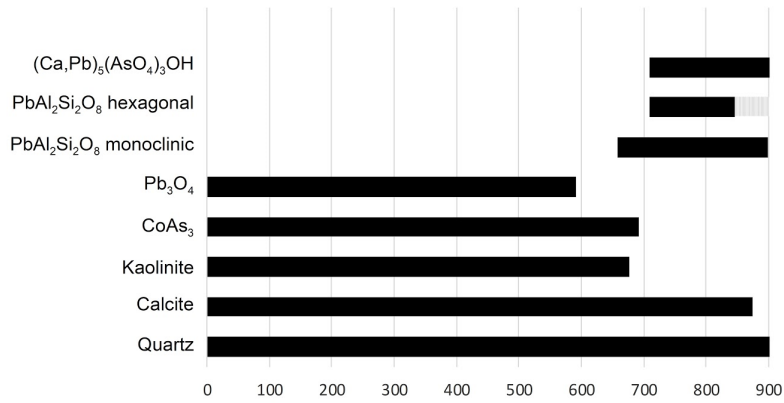
a) m1



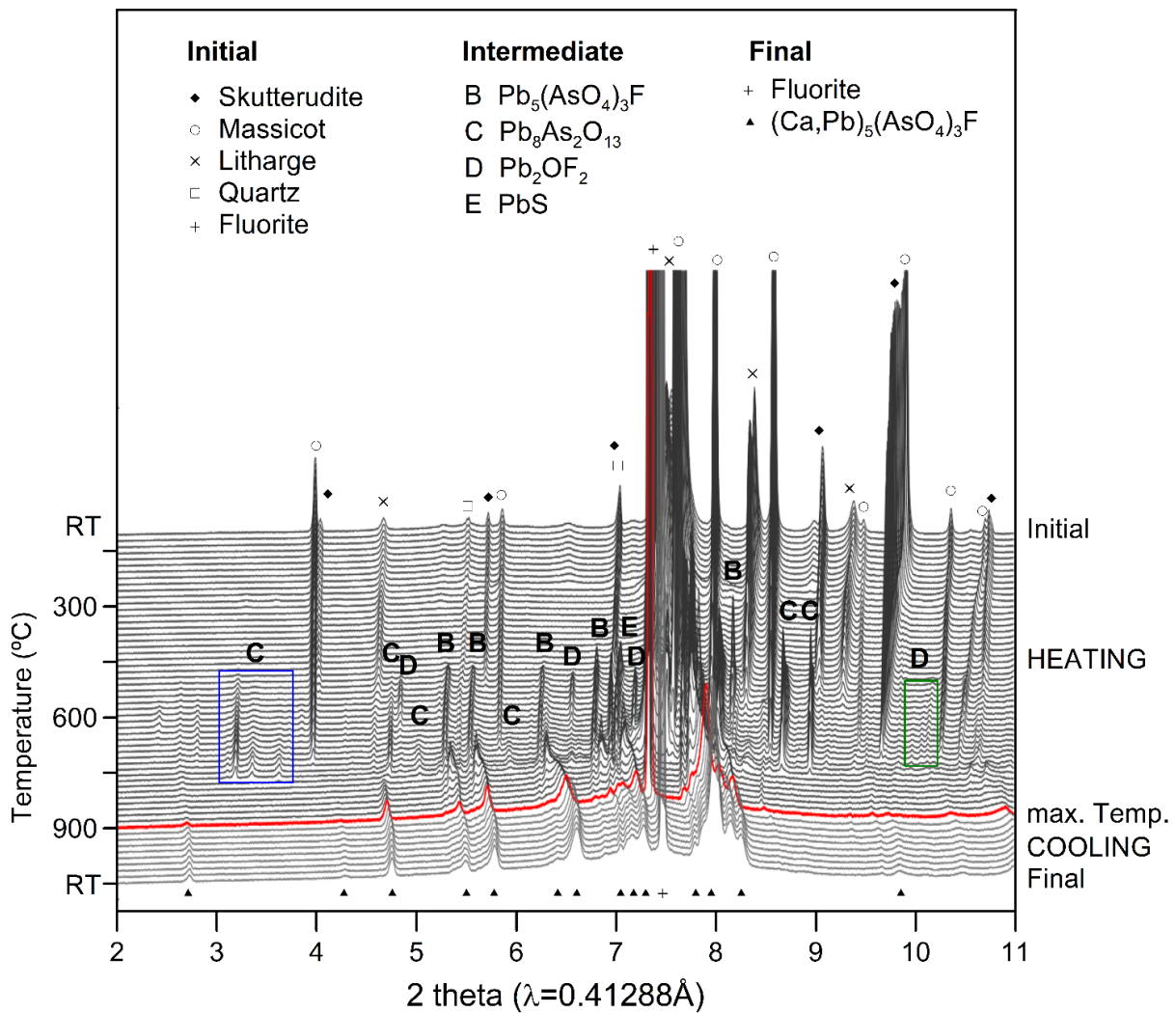
b) m9



c) m16

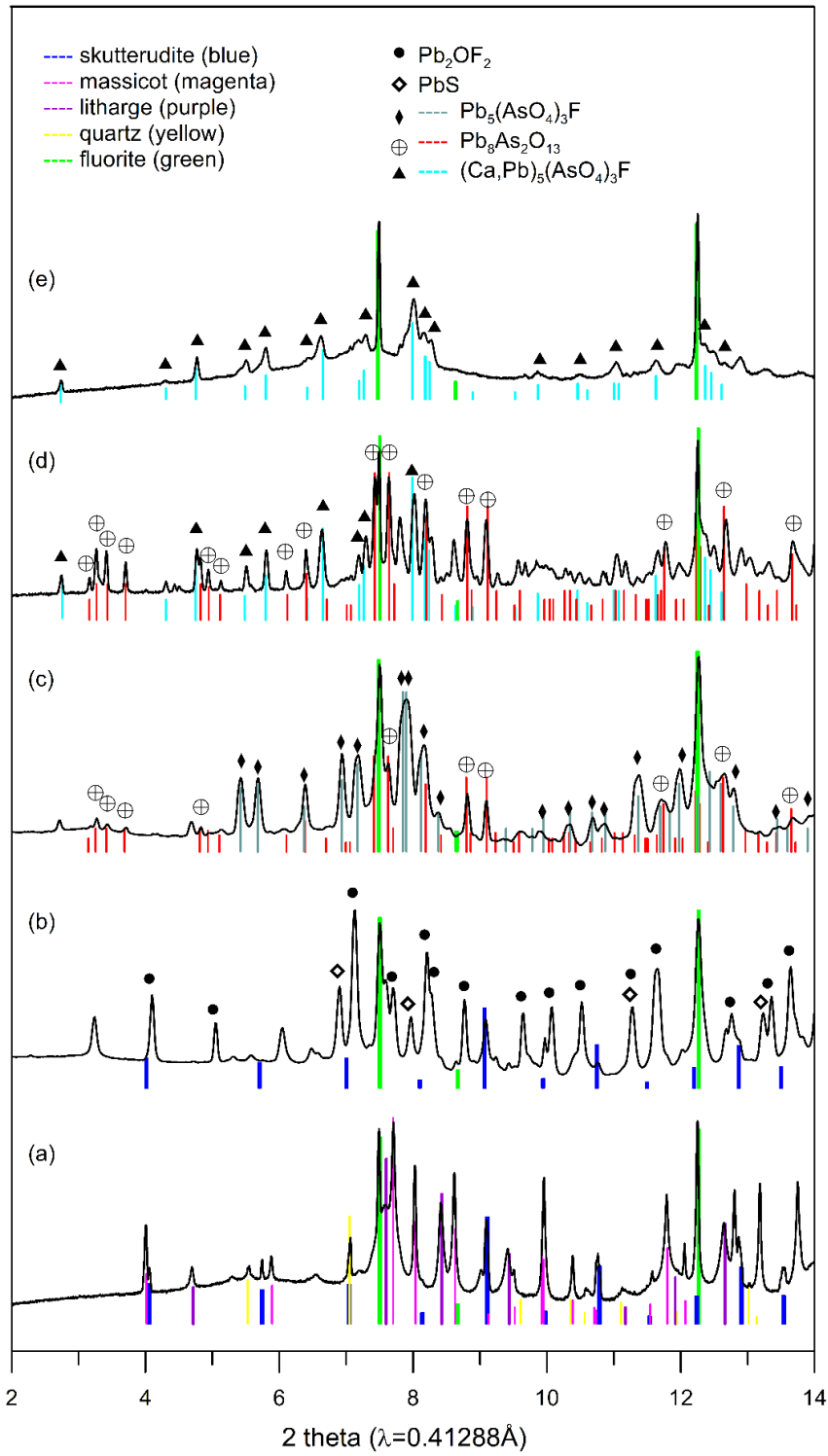


702  
703 **Figure 4.** Thermal stability ranges of phases of m1, m9 and m16.  
704  
705



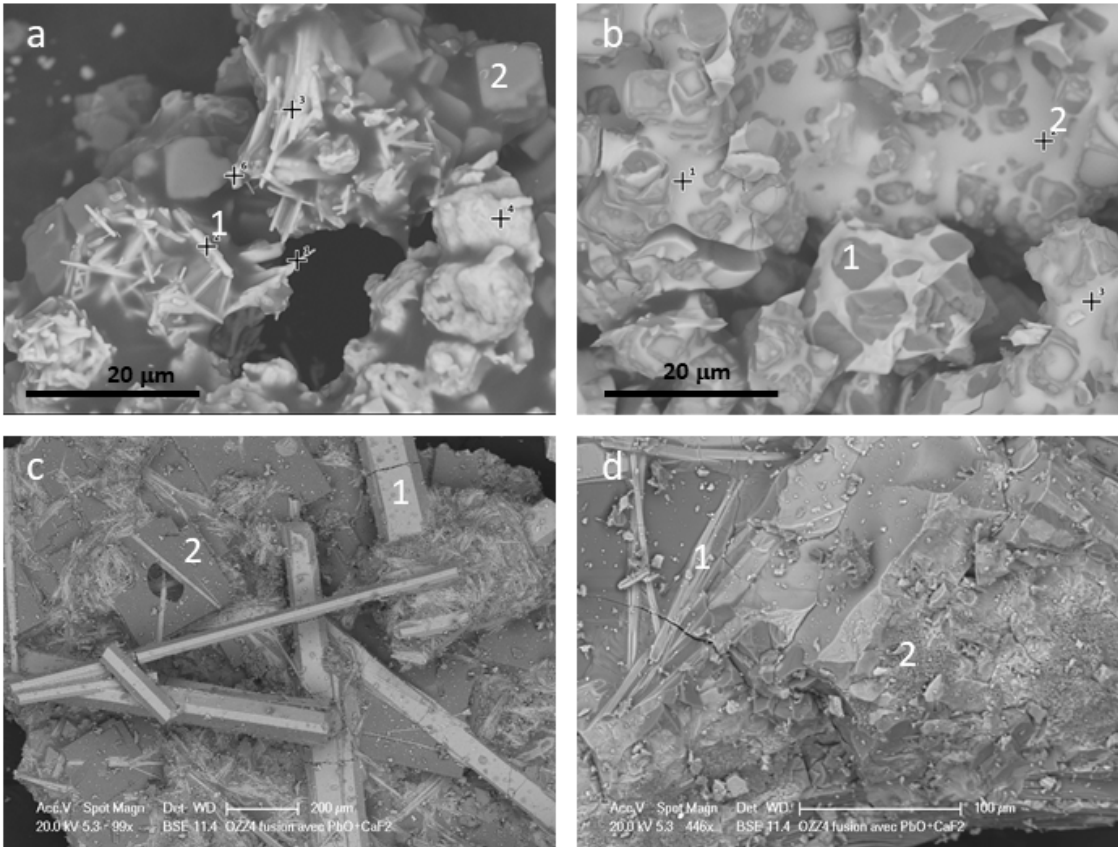
706  
707  
708  
709  
710  
711  
712

**Figure 5.** Diffractogram evolution of mixture m9 (Table I) from room temperature (top pattern) to the maximum temperature of 900 °C (red pattern) and cooling to room temperature (bottom pattern). The mixture components at RT, are identified by the symbols in the legend. The phases formed during the thermal treatment are indicated by the letter B to E.



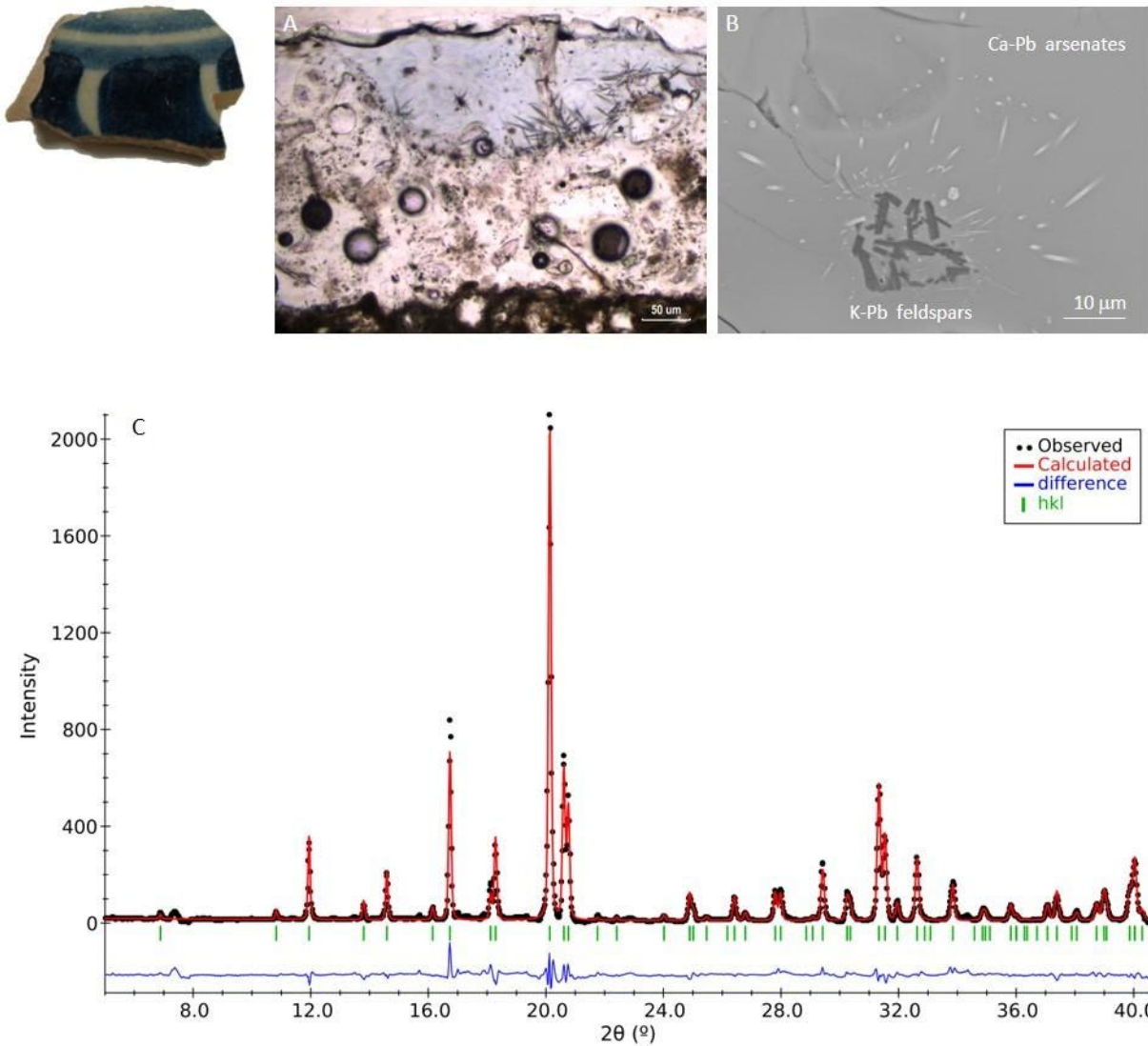
713  
 714  
 715  
 716  
 717  
 718

**Figure 6.** SR-XRD patterns corresponding to the mixture m9 (table I). (a) before heating, (b) external zone of capillary (c) middle zone of capillary, (d) near maximum temperature of capillary (e) zone of maximum heating collected at RT after cooling.



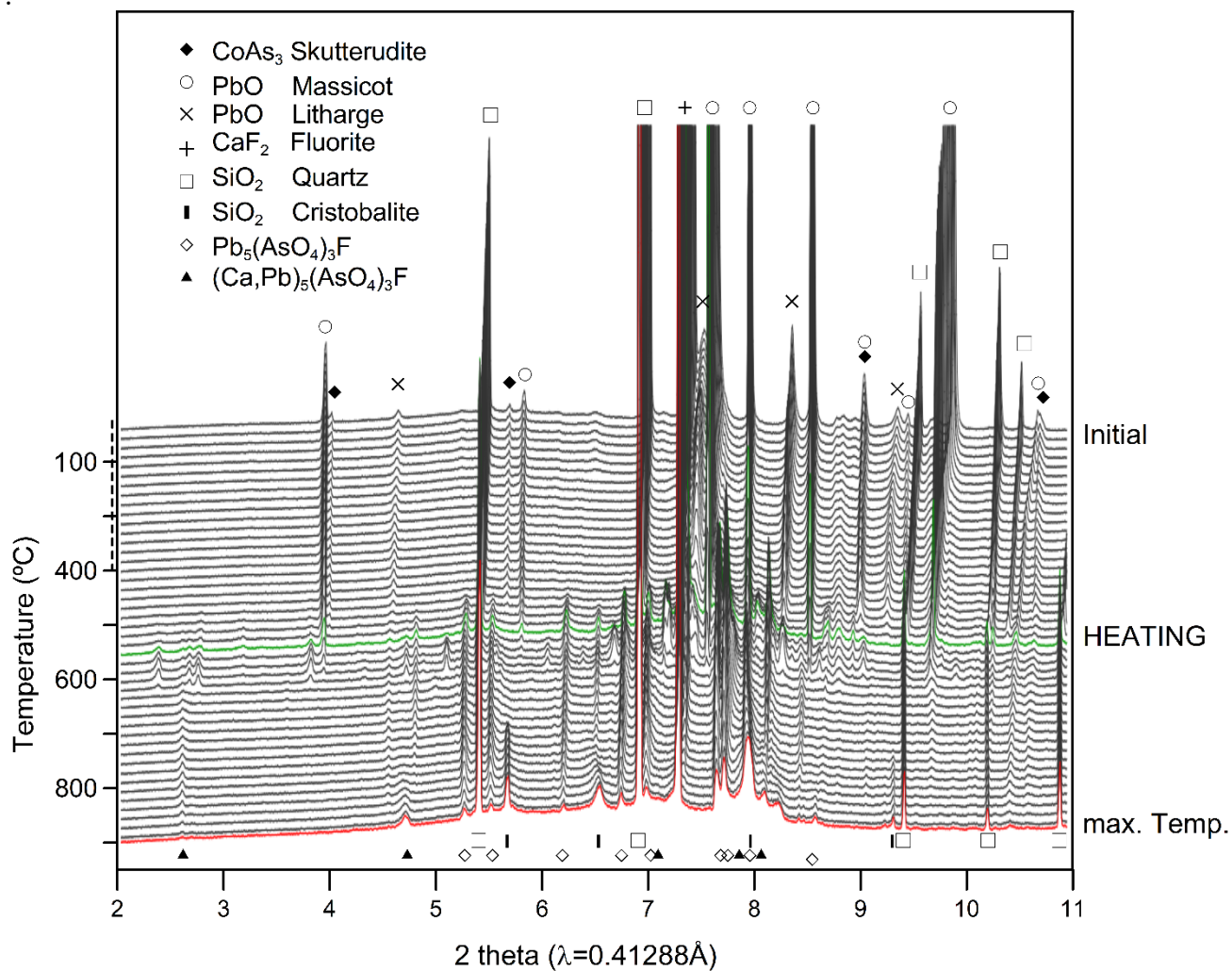
719  
720  
721  
722  
723  
724  
725  
726

**Fig. 7.** SEM images of mixture m9 fired at 900°C (DP) (a) and (b) and 1200°C (c) and (d) (SP).  
 a) Lead arsenate tiny crystals (1) grown over cubes of fluorite (2).  
 b) Fluorite crystals (1) surrounded by lead rich vitreous phase (2).  
 c) Calcium arsenate crystals (1) and calcium aluminosilicate crystallites (anorthite type) (2).  
 d) Calcium arsenates crystals (1) and aggregates of tiny crystals rich in cobalt, iron and nickel (2)



727  
728  
729  
730  
731  
732  
733

**Figure 8.** A) Thin section of blue decorated Catalan glaze from 18th century (SBG17). The blue decoration was applied overglaze. The Ca-Pb arsenates acicular crystals are formed in the contact between tin lead glaze and blue decoration layer. B) SEM BSE image of Ca-Pb arsenates (white colour) and lead feldspars (grey colour). C) Rietveld refinement of the Ca-Pb arsenate apatite-like structure.



735

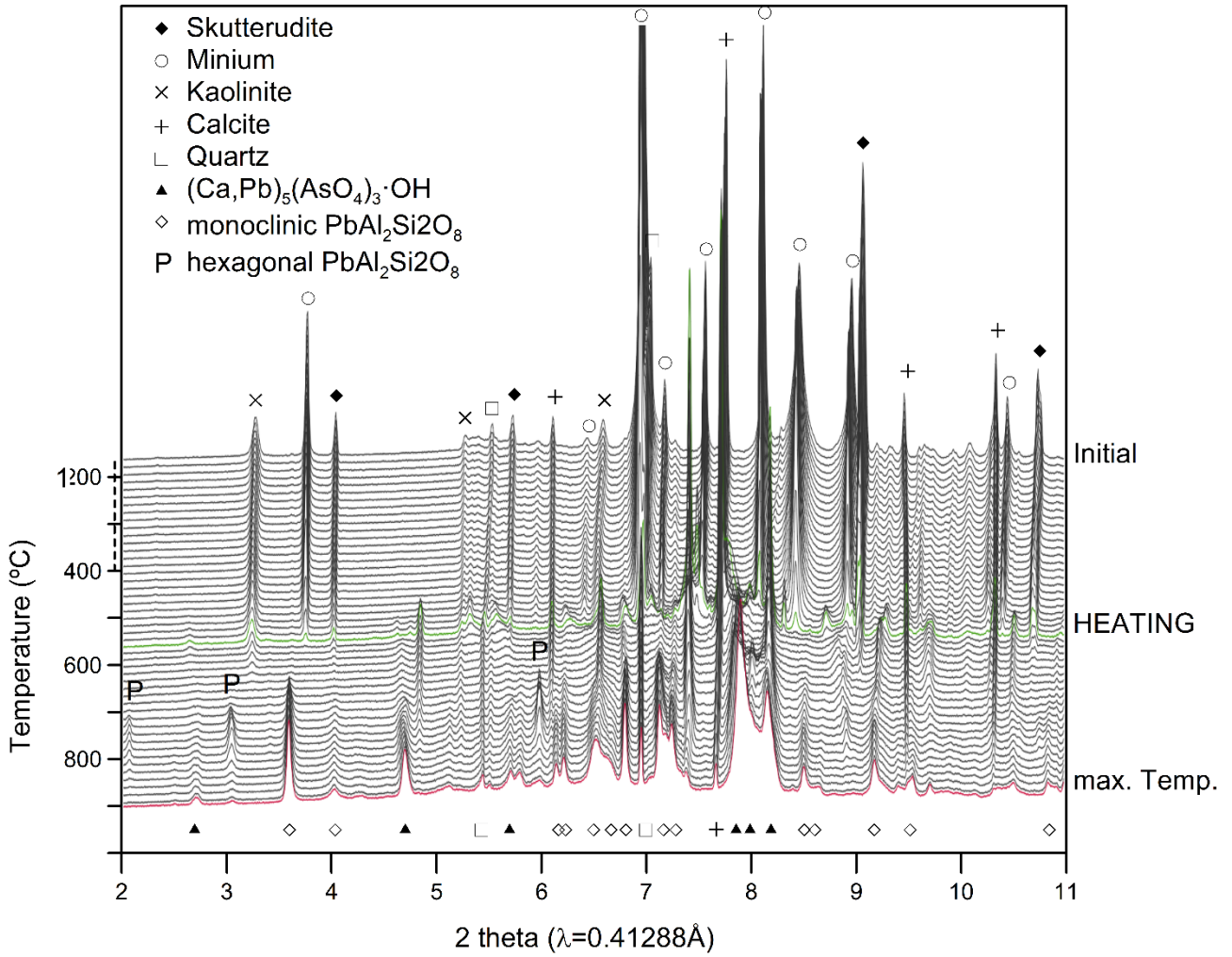
736 **Figure 9.** Diffractogram evolution of mixture m11 (table I) from room temperature (top pattern) to

737 the maximum temperature of 900 °C (red pattern). Green diffractogram corresponds to 573 °C

738 (quartz alpha to quartz beta transition).

739





740  
741  
742  
743  
744  
745  
746  
747  
748  
749

**Figure 10.** Diffractogram evolution of mixture **m16** (table I) from room temperature (top pattern) to the maximum temperature of 900 °C (red pattern). Green diffractogram corresponds to 573 °C (quartz alpha to quartz beta transition).